

Refereed article

## Investigation of optical and near-infrared surface brightness profiles of spiral galaxies\*

Barbara Cunow

Department of Mathematics, Applied Mathematics and Astronomy,  
University of South Africa, PO Box 392, Pretoria 0003, South Africa  
cunowbhl@unisa.ac.za

**Abstract.** For 32 non-active and 32 Seyfert spiral galaxies, optical and near-infrared surface brightness profiles are measured and the disc scalelengths are determined. It is found for the optical wavelength regions that the non-active galaxies show significant colour gradients within their discs, whereas the Seyfert galaxies do not. In the near-infrared, the observed colour gradients are the same for the non-active and the active galaxies.

A comparison of the optical data with model calculations indicates that the colour gradients in the discs of the non-active galaxies are caused by a combination of an intrinsic colour gradient in the stellar disc and dust extinction. The Seyfert galaxies do not have a colour gradient in the stellar disc and are optically thin throughout the disc.

**Keywords:** galaxies: spiral – galaxies: Seyfert – galaxies: photometry

### 1. Introduction

Galaxies are large objects in the Universe which are made of stars, gas and dust. Spiral galaxies are those galaxies which show a spiral structure. The main components of a spiral galaxy are the bulge, the disc and the halo. The bulge dominates the inner regions of the galaxy and contains stars of intermediate age. The disc dominates the outer regions of the galaxy and consists of a luminous disc with the spiral arms containing the young stars, and a dust disc. One of the properties of dust is its ability to absorb light in the ultraviolet, optical and near-infrared wavelength regions. Hence a certain percentage of the light emitted in a galaxy is lost by dust extinction inside the galaxy. In many edge-on galaxies the dust disc is visible as a dark lane. The halo is found above and below the plane of the galaxy outside the bulge and contains old stars. Its surface brightness is normally so much lower than that of the bulge and the disc that it can be neglected.

In most galaxies, all energy output is due to radiation by stars. Such galaxies are called “normal” or “non-active”. However, there are a large number of galaxies with an active nucleus, powered by a supermassive black hole accreting material from its surroundings. In

---

\*Based on observations collected at the South African Astronomical Observatory, Sutherland, South Africa.

this process a huge amount of energy is released. One class of active galaxies are the Seyfert galaxies, named after the astronomer Carl Seyfert, who recognized them in the 1940s. They have a bright nucleus and a spectrum with strong emission lines. Apart from the active nucleus, a Seyfert galaxy cannot be distinguished from a non-active galaxy.

There are a number of ways to analyse the image of a galaxy. A lot of information can be obtained from the surface brightness profile which is a measure of the light intensity as function of the distance from the centre of the galaxy. Colour profiles are obtained from the surface brightness profiles of different wavelength regions.

Studies have shown that many spiral galaxies have a disc which becomes bluer with increasing radius. It is not clear yet what causes these colour gradients. They could be due to stellar population gradients, where the outer disc regions contain a higher fraction of blue stars than the inner regions. Alternatively, they can be caused by dust. Dusty regions appear reddened, because dust blocks blue light more than red light. We know that the density of the stars in the disc decreases with increasing radius, hence it is reasonable to assume that the dust density shows the same behaviour. This means that the dust extinction should be larger in the inner parts of the disc than in the outer parts, and the inner parts should be more reddened than the outer parts. Therefore, the outer regions of the disc should appear bluer than the inner regions. Finally it is possible that we have a combination of both effects.

In order to find out which explanation is correct, a sample of galaxies of the same physical properties but with different inclination angles, covering the whole range from face-on to edge-on view is needed. The reason is that the variation of the observed colour gradient with inclination angle is different for stellar population gradients and dust extinction.

The purpose of the present study is to investigate the colour gradients of galaxy discs as function of the apparent ellipticity which is a measure of the inclination angle. The galaxy sample includes both non-active and active galaxies, because it is not known yet whether there are differences between the properties of the discs of non-active and active spiral galaxies.

## 2. The data

The sample consists of 32 non-active and 32 Seyfert spiral galaxies. It is identical to the one analysed in Cunow (2001), except the fact that another four active galaxies were added to the sample. The galaxies cover the whole range from face-on to edge-on view. The global properties of the non-active and the active galaxies are similar, hence each subsample can act as a control sample for the other. Details about the selection and the properties of the sample are given in Cunow (2001).

For the sample galaxies, images were taken in the optical  $B$ ,  $V$ ,  $R$  and  $I$  bands, and in the near-infrared  $J$ ,  $H$  and  $K_s$  bands covering a wavelength range from 440nm to 2.1 $\mu$ m. Table 1 gives the mean wavelengths for the different photometric filters. The observations were carried out at the South African Astronomical Observatory (SAAO) at Sutherland. The  $BVRI$  images were obtained with the SAAO and the Dandicam CCD cameras at the 1.0-m telescope. The  $JHK_s$  data were obtained using the Dandicam near-infrared camera at the 1.0-m telescope and the near-infrared camera SIRIUS at the Infrared Survey Facility (IRSF).

Detailed information about the instruments at Sutherland can be found at the SAAO website [<http://www.sao.ac.za>].

The *BVRI* data were taken and reduced as described in Cunow (2001). The near-infrared data consist of a large number of short-exposure images. This is necessary, because the sky is very bright in the near-infrared, and an exposure time which is too long produces a saturated image. In addition to the galaxy images, sky images were taken in order to allow proper sky subtraction. In the reduction process, the sky

images are combined and subtracted from each galaxy image, and the different images of a galaxy are combined to produce a final image. A detailed description of the reduction procedures will be given elsewhere. The photometric calibration was done using the standard star measurements of Carter & Meadows (1995) and Persson et al. (1998). The random scatter between the measured magnitudes and the catalogue magnitudes of the standard stars is  $\sigma = 0.04$  mag, which is similar to the random scatter of the *BVRI* magnitudes (Cunow 2001).

In addition to the data obtained at the SAAO, *JHK<sub>s</sub>* images from the Two Micron All Sky Survey (2MASS) were used. The 2MASS is a project which does a near-infrared survey of the whole sky. It produces *JHK<sub>s</sub>* images which can be downloaded from the Internet [<http://irsa.ipac.caltech.edu>]. The data are reduced already, hence no further reduction and/or calibration is necessary. Details about this project are given in Jarrett et al. (2000).

### 3. Data analysis

#### 3.1 Apparent ellipticities

For each galaxy, the apparent ellipticity  $\epsilon$  was measured. It is defined as:

$$\epsilon = 1 - b/a,$$

where  $a$  is the apparent semimajor axis and  $b$  the apparent semiminor axis of the galaxy. Thus we have  $\epsilon = 0$  for a circle and  $\epsilon = 1$  for a line.

The inclination angle  $i$  of a galaxy is the angle between the line perpendicular to the plane of the galaxy and the line of sight. If we see a spiral galaxy face-on, our line of sight is perpendicular to the plane of the galaxy disc, which gives  $i = 0^\circ$ . A face-on spiral appears round, hence we have  $\epsilon = 0$ . The larger the inclination angle, the more elongated appears the galaxy and the larger is  $\epsilon$ . Edge-on spirals have  $i = 90^\circ$  and  $\epsilon \approx 0.85$ .

The apparent ellipticities of the sample galaxies are obtained by using the apparent semimajor and semiminor axes  $a$  and  $b$  from the  $I$  images. Details are given in Cunow (2001).

Table 1. Mean wavelength  $\lambda_0$  for the photometric filters used in this work.

| Filter         | $\lambda_0$ (nm) |
|----------------|------------------|
| B              | 440              |
| V              | 550              |
| R              | 660              |
| I              | 790              |
| J              | 1250             |
| H              | 1650             |
| K <sub>s</sub> | 2100             |

### 3.2 Disc scalelengths

For each galaxy and filter, surface brightness profiles were measured, with the surface brightness given in  $\text{mag} \cdot \text{arcsec}^{-2}$ . The profile is obtained by dividing the galaxy image into a large number of intensity intervals and fitting an ellipse to each interval. The radius is measured along the semimajor axis. An example of such a profile is given in Figure 1 of Cunow (1998).

The light distribution of a galaxy disc can be approximated by an exponential law. Since the astronomical magnitude is a logarithmic scale, surface brightness profiles following an exponential law are linear. The fit is done using the relation:

$$F = F_0 \exp(-r/r_D),$$

where  $F$  is the flux per solid angle,  $r$  the radius along the semimajor axis and  $r_D$  the disc scalelength.

Disc scalelengths were determined for each galaxy and filter by using the linear parts of the surface brightness profiles outside the bulge. The measurement error for  $r_D$  is  $\sigma(r_D) \approx 10\%$  for  $BVRI$  and  $\sigma(r_D) = 15\%$  for  $JHK_s$ . More details are found in Cunow (1998, 2001).

### 3.3 Colour gradients

The disc scalelength is a parameter which describes how flat or steep a surface brightness profile is. The larger  $r_D$ , the flatter is the profile. The colour gradients are given by the ratio of the disc scalelengths of different wavelength regions. If  $r_D(F_1)/r_D(F_2)$  is the scalelength ratio of a galaxy for wavelength bands  $F_1$  and  $F_2$  and if  $F_1$  covers a bluer wavelength region than  $F_2$ , we have:

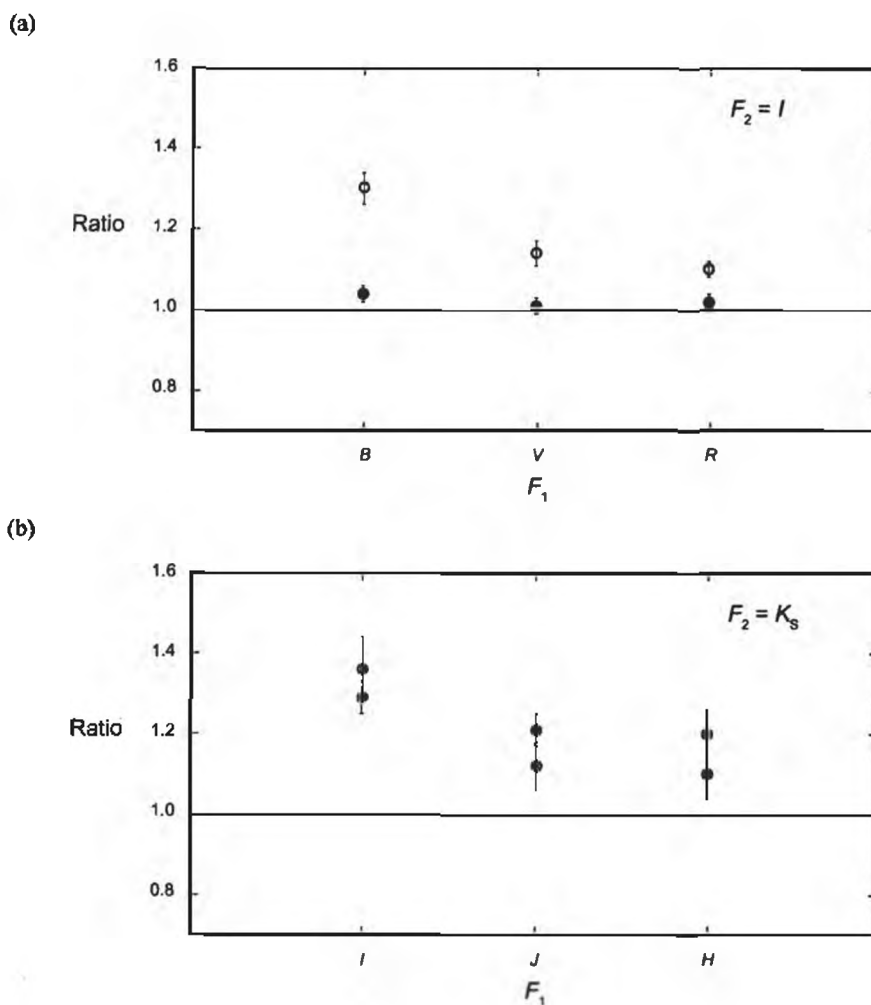
- $r_D(F_1)/r_D(F_2) = 1$ : The disc colour does not change with radius, i.e. no colour gradient.
- $r_D(F_1)/r_D(F_2) > 1$ : The outer parts of the disc are bluer than the inner parts.
- $r_D(F_1)/r_D(F_2) < 1$ : The outer parts of the disc are redder than the inner parts.

Hence the variation of  $r_D(F_1)/r_D(F_2)$  with  $\epsilon$  can be used to study the variation of the colour gradients with inclination angle.

## 3.4 Results

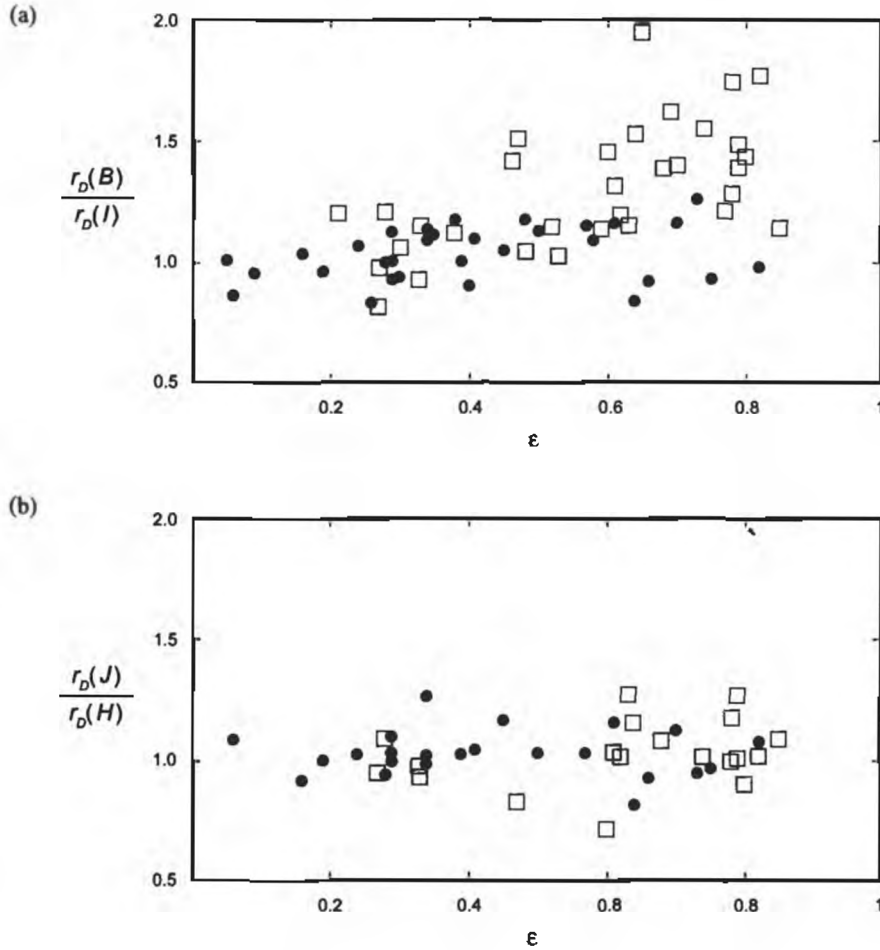
### 3.4.1 Average scalelength ratios

Figure 1 shows the average scalelength ratios. Figure 1a shows the optical ratios, Figure 1b the near-infrared ones. In the optical wavelength regions, the non-active galaxies show significant colour gradients within their discs (the outer parts are bluer than the inner parts), whereas the active galaxies do not. In the near-infrared wavelength regions, colour gradients are present for both the non-active and the active galaxies. The differences between the non-active and the active galaxies seen in the optical regions are not present in the near-infrared.



**Figure 1.** Average scalelength ratios  $\langle r_D(F_1)/r_D(F_2) \rangle$  for the sample galaxies. The open symbols denote the non-active galaxies, whereas the filled symbols denote the active galaxies. (a) shows the optical ratios with  $F_2 = I$ , (b) shows the near-infrared ratios with  $F_2 = K_s$ .

The  $JHK_s$  scalelengths are significantly shorter than  $r_D(I)$ , and the  $K_s$  scalelengths are clearly shorter than  $r_D(J)$  and  $r_D(H)$ . However, it is difficult to say whether the differences between the  $JH$  scalelengths and  $r_D(K_s)$  are significant. For  $J$  and  $H$  we find that  $\langle r_D(J)/r_D(H) \rangle = 1.02 \pm 0.03$  for the non-active galaxies and  $\langle r_D(J)/r_D(H) \rangle = 1.03 \pm 0.02$  for the active galaxies. Hence no colour gradients exist for  $J-H$ .



**Figure 2.** Disc scalelength ratios plotted against apparent ellipticity  $\epsilon$ . (a) shows the ratios between  $B$  and  $I$ , (b) shows the ratios between  $J$  and  $H$ . The non-active galaxies are denoted by  $\square$ , the active galaxies by  $\bullet$ .

### 3.4.2 Scalelength ratios at different inclination angles

Figure 2 shows two examples for  $r_D(F_1)/r_D(F_2)$  plotted against  $\epsilon$ . Figure 2a shows  $r_D(B)/r_D(I)$ , Figure 2b  $r_D(J)/r_D(H)$ . For the non-active galaxies,  $r_D(B)/r_D(I)$  increases from 1.0 for face-on galaxies to 1.5 for edge-on galaxies, which means that the edge-on galaxies have larger colour gradients than the face-on ones, but  $r_D(J)/r_D(H) \approx 1$  for all inclination angles. For the active galaxies, neither  $r_D(B)/r_D(I)$  nor  $r_D(J)/r_D(H)$  changes systematically with increasing  $\epsilon$ .

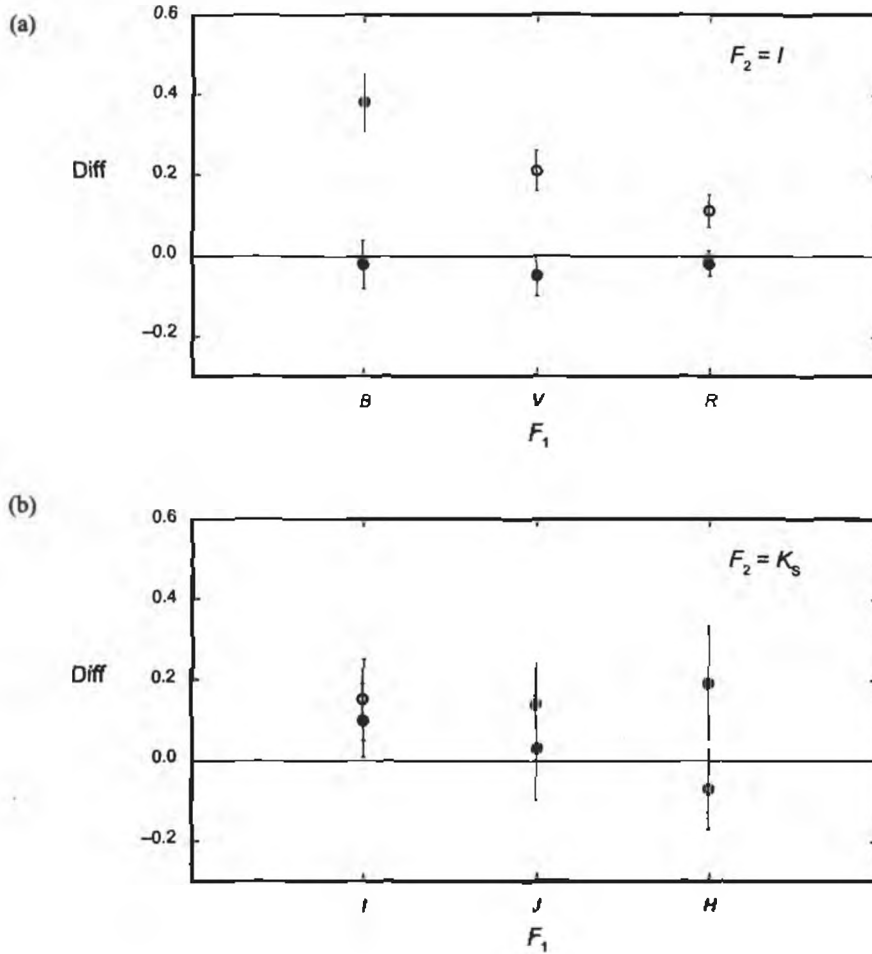


Figure 3. Difference between average scalelength ratios  $\langle r_D(F_1)/r_D(F_2) \rangle$  for galaxies with  $\epsilon \geq 0.6$  and those for galaxies with  $\epsilon \leq 0.4$ . The open symbols denote the non-active galaxies, whereas the filled symbols denote the active galaxies. (a) shows the optical differences with  $F_2 = I$ , (b) shows the near-infrared differences with  $F_2 = K_s$ .  
 Diff =  $\langle r_D(F_1)/r_D(F_2) \rangle (\epsilon \geq 0.6) - \langle r_D(F_1)/r_D(F_2) \rangle (\epsilon \leq 0.4)$ .

Figure 3 shows the differences between  $\langle r_D(F_1)/r_D(F_2) \rangle$  for the galaxies with  $\epsilon \geq 0.6$  and  $\langle r_D(F_1)/r_D(F_2) \rangle$  for the galaxies with  $\epsilon \leq 0.4$ . These differences are a convenient measure for the change of  $r_D(F_1)/r_D(F_2)$  with increasing  $\epsilon$ . In the optical wavelength regions, the colour gradients of the non-active galaxies with large ellipticities are significantly larger than

Reproduced by Subinset Gateway under license granted by the Publisher (dated 2013.)

those of the non-active galaxies with small ellipticities, whereas for the active galaxies no colour gradients exist, neither for the face-on galaxies, nor for the edge-on galaxies. In the near-infrared wavelength regions, the colour gradients are the same for the face-on and the edge-on galaxies, and no significant differences exist between the non-active and the active galaxies.

#### 4 Comparison with models

##### 4.1 The models

In order to determine whether the observed colour gradients are caused by colour gradients in the stellar disc or by dust extinction or by a combination of both effects, the data are compared with scalelength ratios obtained from images of model galaxies.

At present, model images in *BVRI* have been calculated. The model galaxies consist of a bulge, a luminous stellar disc and an absorbing dust disc. Two sets of models are used, (i) model galaxies without a colour gradient in the stellar disc, and (ii) model galaxies for which the outer parts of the stellar disc are bluer than the inner parts. The calculations were done for a variety of inclination angles and optical depths. The optical depth  $\tau$  is a measure of the dust content of a galaxy. The larger  $\tau$ , the more dust is present. A dust-free galaxy has  $\tau = 0$ .

For the inclination angle  $i$ , the following values were adopted:  $0^\circ$ ,  $20^\circ$ ,  $40^\circ$ ,  $60^\circ$ ,  $70^\circ$ ,  $80^\circ$  and  $84^\circ$ . For the central face-on optical depth in the *B* band,  $\tau_0^B = 0$ ; 0.5; 1; 3; 5; 7; 10 was used. A detailed description of the model calculations is given in Cunow (2001).

The model images are analysed in the same way as the data of the real galaxies. For each model galaxy, the apparent ellipticity and the *BVRI* disc scalelengths are determined as described in Section 3.

Figure 4 shows the disc scalelength ratios plotted against apparent ellipticity  $\epsilon$  for

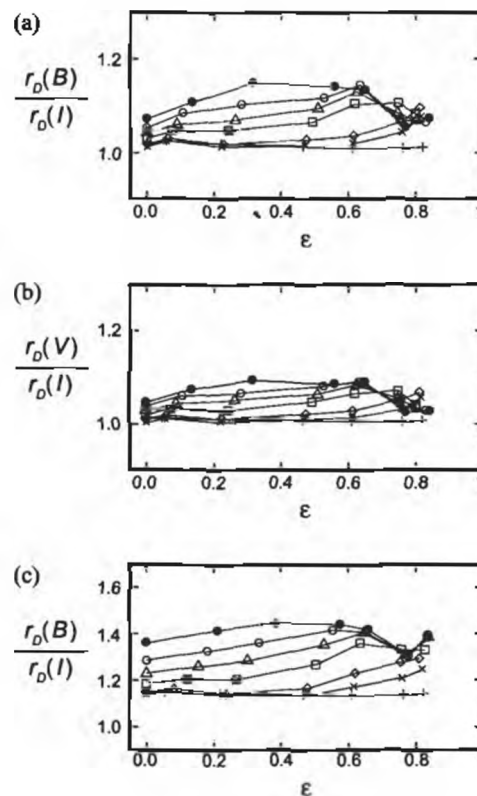


Figure 4. Disc scalelength ratios plotted against apparent ellipticity  $\epsilon$  for the models. (a) and (b) show a model without a colour gradient in the stellar disc, whereas (c) shows a model with a colour gradient.

Optical depth: + for  $\tau_0^B = 0$ , x for  $\tau_0^B = 0.5$ ,  $\diamond$  for  $\tau_0^B = 1$ ,  $\square$  for  $\tau_0^B = 3$ ,  $\triangle$  for  $\tau_0^B = 5$ ,  $\circ$  for  $\tau_0^B = 7$ , and  $\bullet$  for  $\tau_0^B = 10$ .

the models. Figures 4a and 4b show a model without a colour gradient in the stellar disc, whereas Figure 4c shows a model with a colour gradient.

The main features of the scalelength ratios  $r_D(F_1)/r_D(F_2)$  from the models are the following:

- The larger the optical depth, the larger is  $r_D(F_1)/r_D(F_2)$ .
- The smaller the wavelength difference between  $F_1$  and  $F_2$ , the smaller is the increase of  $r_D(F_1)/r_D(F_2)$  with increasing  $\tau_0^B$ .
- For a dust-free galaxy,  $r_D(F_1)/r_D(F_2) = 1$  if there is no colour gradient in the stellar disc, and  $r_D(F_1)/r_D(F_2) > 1$  if the outer parts of the stellar disc are bluer than the inner parts.

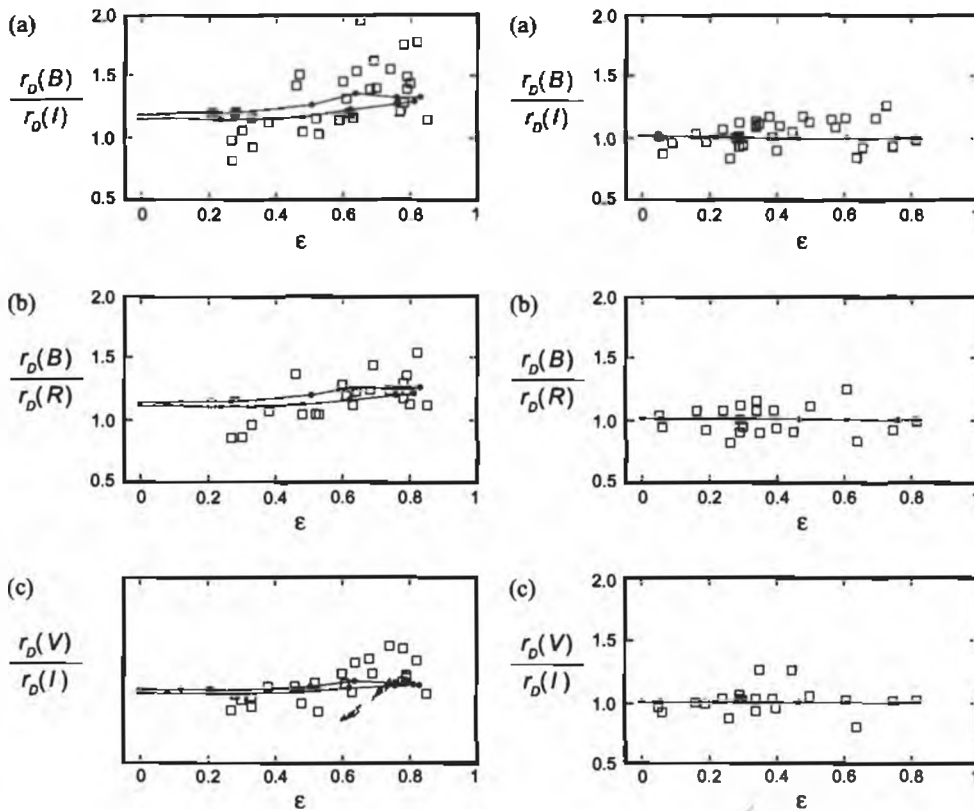


**Figure 5.** Disc scalelength ratios plotted against apparent ellipticity  $\epsilon$  for the non-active galaxies. The lines show the best-fitting models with  $\tau_0^B = 1$  (lower curve) and  $\tau_0^B = 3$  (upper curve).

**Figure 6.** Disc scalelength ratios plotted against apparent ellipticity  $\epsilon$  for the active galaxies. The line shows the best-fitting model.

- For an intermediate optical depth,  $r_D(F_1)/r_D(F_2)$  increases systematically from face-on to edge-on view.

#### 4.2 Results

The model data are compared with the data of the real galaxies by using  $r_D(B)/r_D(I)$ ,  $r_D(B)/r_D(R)$  and  $r_D(V)/r_D(I)$ . The ratios  $r_D(B)/r_D(V)$ ,  $r_D(V)/r_D(R)$  and  $r_D(R)/r_D(I)$  are not used, because the variation of the scalelength ratios with changing optical depth is so small that the fit is dominated by the scatter of the data.

For the non-active galaxies, the  $r_D(B)/r_D(I)$  data are fitted best with a model with a colour gradient in the stellar disc and an optical depth of  $\tau_0^B = 3$ . If  $r_D(V)/r_D(I)$  and  $r_D(B)/r_D(R)$  are included also, the result is the same, but the fit for  $\tau_0^B = 1$  is almost as good as the one for  $\tau_0^B = 3$ . The models with no colour gradient in the stellar disc do not fit the data. This means that the colour gradients observed in the discs of the non-active galaxies are caused by a combination of a colour gradient within the stellar disc and dust extinction. The galaxies show significant extinction in the centre, but they are optically thin in the outer regions (see Cunow 2001). Figure 5 shows the data and the best-fitting model.

For the active galaxies, the data are fitted best by a model with no colour gradient in the stellar disc and no dust ( $\tau_0^B = 0$ ), which means that they are optically thin throughout the disc. Figure 6 shows the data and the best-fitting model.

#### 5 Conclusions

The results of this work can be summarized as follows:

- Optical data:
  - Non-active spiral galaxies show significant colour gradients in their discs which increase systematically from face-on to edge-on view, whereas active spiral galaxies do not.
  - The comparison with model calculations indicates that the colour gradients in the discs of non-active galaxies are caused by a combination of an intrinsic colour gradient in the stellar disc and dust extinction. Active galaxies are optically thin and no intrinsic colour gradient exists in the stellar disc.
  - The above results indicate that structural differences exist between the discs of non-active and active spiral galaxies.
- Near-infrared data:
  - Colour gradients are observed in both the non-active and the active galaxies. However, it is difficult to say whether they are significant.
  - The colour gradients do not vary from face-on to edge-on view, neither for the non-active galaxies, nor for the active galaxies.
  - There are no differences between the colour gradients of the non-active and the active galaxies. Hence the differences found in the optical wavelength regions do not exist in the near-infrared.

### **Acknowledgements**

I thank the South African Astronomical Observatory for allocation of observing time at Sutherland. The IRSF is a joint project of the SAAO and the University of Nagoya/Japan, and I thank the programme committee for allocation of observing time at the IRSF. Furthermore, I thank the South African National Research Foundation (NRF) for financial support of this project. This research has made use of the MIDAS software supplied by ESO, of the Two Micron All Sky Survey (2MASS) which is a joint project of the University of Massachusetts and the Infrared Processing and Analysis Center, California, USA, of the Simbad database at CDS, Strasbourg, France, and of the Lyon-Meudon Extragalactic Database (LEDA) supplied by the LEDA team at the Observatoire de Lyon.

### **References**

- Carter B.S. & Meadows V.S. (1995) Fainter Southern JHK Standards Suitable for Infrared Arrays. *Monthly Notices of the Royal Astronomical Society*, 276, 734.
- Cunow B. (1998) Surface Photometry of Normal and Active Spiral Galaxies. *Monthly Notes of the Astronomical Society of Southern Africa*, 57 (9 & 10), 52.
- Cunow B. (2001) Disc scalelengths of non-active and active spiral galaxies. *Monthly Notices of the Royal Astronomical Society*, 323, 130.
- Jarrett T.H., Chester T., Cutri R., Schneider S., Skrutskie M. & Huchra J.P. (2000) 2MASS Extended Source Catalog: Overview and Algorithms. *Astronomical Journal*, 119, 2498.
- Persson S.E., Murphy D.C., Krzeminski W., Roth M. & Rieke M.J. (1998) A New System of Faint Near-Infrared Standard Stars. *Astronomical Journal*, 116, 2475.